THE JOURNAL OF BIOLOGICAL CHEMISTRY
Vol. 280, No. 7, Issue of February 18, pp. 6064–6071, 2005

Printed in U.S.A.

Changes in Mg^{2+} Ion Concentration and Heavy Chain Phosphorylation Regulate the Motor Activity of a Class I Myosin*

Received for publication, November 4, 2004, and in revised form, November 26, 2004
Published, JBC Papers in Press, December 4, 2004, DOI 10.1074/jbc.M412473200

Setsuko Fujita-Becker‡§, Ulrike Dürrwang‡§¶, Muriel Erent‡‖, Richard J. Clark, Michael A. Geeves**, and Dietmar J. Manstein‡ ‡‡ §§**

*From the ‡Department of Biophysics, Max-Planck-Institute for Medical Research, Jahnstrasse 29, D-69120 Heidelberg, Germany, the **Department of Biosciences, University of Kent, Canterbury CT2 7NJ, United Kingdom, and the ‡‡Institute for Biophysical Chemistry, OE 4350, Hannover Medical School, Carl-Neuberg-Strasse 1, D-30623 Hannover, Germany*

Class I myosins are single-headed motor proteins implicated in various motile processes including organelle translocation, ion channel gating, and cytoskeleton reorganization. *Dictyostelium discoideum* myosin-ID belongs to subclass 1α, whose members are thought to be tuned for rapid sliding. The direct analysis of myosin-ID motor activity is made possible by the production of single polypeptide constructs carrying an artificial lever arm. Using these constructs, we show that the motor activity of myosin-ID is activated 80-fold by phosphorylation at the TEDS site. TEDS site phosphorylation acts by stabilizing the actomyosin complex and increasing the coupling between actin binding and the release of hydrolysis products. A surprising effect of Mg^{2+} ions on *in vitro* motility was discovered. Changes in the level of free Mg^{2+} ions within the physiological range are shown to modulate motor activity by inhibiting ADP release. Our results indicate that higher concentrations of free Mg^{2+} ions stabilize the tension-bearing actin myosin ADP state and shift the system from the production of rapid movement toward the generation of tension.

Class I myosins are produced by a wide range of organisms and cell types (1). They share a conserved motor domain, a light chain-binding domain, and a tail region that contains a polybasic region that directly binds to membranes via electrostatic interactions (2, 3). Phylogenetic analysis reveals that there are at least four myosin I subclasses. *Dictyostelium discoideum* myosin-ID is a member of the amoeboid subclass. Despite its name, this is the most widely expressed subclass. Amoeboid class I myosins have two additional domains in their tails that are involved in ATP-insensitive actin binding. The first domain is a region rich in the amino acids glycine, serine, and alanine (or glutamate or serine) (4–6), and the second domain is a Src homology 3 domain (7, 8).

The regulation of class I myosins from a wide range of organisms appears to be mediated by the phosphorylation of a serine or threonine residue in the motor domain that is located 16 residues upstream of the highly conserved DALAK sequence. Vertebrate class I myosins, like nearly all other myosins, have negatively charged glutamate or aspartate residues at the corresponding position. Therefore the phosphorylation site is generally referred to as the TEDS site (9). The TEDS site resides in a surface loop that forms part of the actin-binding site. The heavy chain of myosin-ID is an *in vitro* substrate for members of the p21-activated kinase/STE20 family of protein kinases (10–13). p21-activated kinases become activated by interaction with lipids and the GTP-bound forms of Rac and Cdc42, leading to reduced inhibition of the catalytic domain by the regulatory domain (14). Although the importance of TEDS site phosphorylation for the kinetic behavior and *in vivo* function of class I myosins is well documented, the direct effect of TEDS site phosphorylation on the motile activity of class I myosins is less well understood. Here, we generated three types of recombinant constructs to analyze the functional properties of *D. discoideum* myosin-ID. Motor domain constructs were used to determine steady-state and transient kinetic parameters. To directly measure the motor activity of myosin-ID, we generated a motor domain fragment with an artificial lever arm consisting of *D. discoideum* α-actinin repeats 1 and 2 (15, 16). The terminology used (D692 and D692–2R) refers to the type of myosin-I and the site of motor domain truncation. 2R serves as abbreviation for the attachment of two α-actinin repeats to the motor domain. To study the effects of the TEDS site phosphorylation on the motor properties, we generated the dephosphorylated and phosphorylated forms of D692–2R by treatment with λ-phosphatase and *Acanthamoeba castellanii* myosin-I heavy chain kinase (17). Additionally, we generated mutant versions of D692–2R, which facilitated the combined characterization of motor and kinetic properties. The serine at the TEDS site of these constructs was replaced by either an alanine residue, to mimic the unphosphorylated state, or a glutamate residue, to mimic the phosphorylated state (18, 19). These constructs are referred to as S332A or S332E mutants in the following text.

EXPERIMENTAL PROCEDURES

Reagents—Standard chemicals were purchased from Sigma, and restriction enzymes, polymerases, and DNA-modifying enzymes were from Roche Applied Science. TRITC-labeled[1] phalloidin was a gift from Dr. H. Faulstich (20).

Cell Growth and Transformation—Dictyostelium cells were grown in

* This work was supported by Deutsche Forschungsgemeinschaft Grants MA1081/5-3 and MA1082/6-1 (to D. J. M.) and Wellcome Trust Grant 070021 (to M. A. G.). The costs of publication of this article were defrayed in part by the payment of page charges. This article must therefore be hereby marked "*advertisement*" in accordance with 18 U.S.C. Section 1734 solely to indicate this fact.

§ These authors contributed equally to this work.
¶ Present address: Marie Curie Research Institute, The Chart, Oxted RH8 OTE Surrey, UK.
‖ Present address: Biochemie-Zentrum der Universität Heidelberg, Im Neuenheimer Feld 328, 69120 Heidelberg, Germany.
§§ To whom correspondence should be addressed: Institut für Biophysikalische Chemie, OE 4350, Medizinische Hochschule Hannover, Carl-Neuberg-Strasse 1, D-30623 Hannover, Germany. Tel.: 49-511-5323700; Fax: 49-511-532–5966; E-mail: manstein@bpc.mh-hannover.de.

[1] The abbreviations used are: TRITC, tetramethylrhodamine isothiocyanate; MlcD, *D. discoideum* myosin-ID light chain; MOPS, 4-morpholinepropanesulfonic acid.

HL-5C medium (21). The cells were transformed by electroporation (22). G418 was used as selectable marker at 10 μg/μl.

Plasmid Constructs and Mutagenesis—Genomic DNA was isolated from AX2 cells according to Ref. 23. PCR-directed mutagenesis was used to isolate *myoD* gene fragments encoding the motor domains with a unique BamHI site at the 5′-end of the coding region and a unique XhoI site at position 692. The PCR products were digested with BamHI and XhoI and cloned into pDXA-3H (24), which carries sequences for the fusion of a C-terminal His_8 tag. The resulting plasmids were analyzed by sequencing. For the production of motor domain constructs fused to two *D. discoideum* α-actinin repeats (2R), a DNA fragment encoding 2R, a Gly-Ser-Gly-Gly-Ser-Gly-Gly-Ser-Gly-Gly-Ser-Gly linker, enhanced yellow fluorescent protein, and a His_8 tag was obtained as XhoI/SphI fragment from pM790–2R-EYFP (25) and inserted in the XhoI/SphI-digested myosin-ID motor domain expression plasmid.

Direct Functional Assays—Actin sliding motility was measured as described previously (15, 26). TEDS site phosphorylation was performed by mixing 1 mg/ml D692–2R with 0.027 mg/ml activated kinase and incubation in the presence of 1 mM EGTA, 3 mM $MgCl_2$, and 2 mM ATP at 30 °C for 20 min. *A. castellanii* myosin-I heavy chain kinase was activated by autophosphorylation at 30 °C for 20 min in a buffer containing 100 mM imidazole, pH 7.0, 4 mM ATP, 6 mM $MgCl_2$, and 2 mM EGTA (12). *A. castellanii* myosin-I heavy chain kinase was generously provided by Drs. E. D. Korn and H. Brzeska (Laboratory of Cell Biology, NHLBI, National Institutes of Health). Dephosphorylation was performed by incubation of 1 mg/ml D692–2R with 4000 units/ml λ-protein phosphatase in the presence of 4 mM dithiothreitol, 2 mM $MnCl_2$, and 0.01% Brij 35 at 30 °C for 30 min.

Kinetic Measurements—Stopped flow measurements were performed at 20 °C with a Hi-tech Scientific SF-61 DX2 double mixing stopped flow system using the procedures and kinetic models described previously (27–30). The binding and hydrolysis of ATP by myosin-ID head fragments were analyzed in terms of the seven-step model (see Scheme 1) described by Bagshaw *et al.* (31). Transients in the presence of actin were analyzed in terms of Schemes 2 and 3 (32, 33). Steady-state ATPase activities were measured at 25 °C with the NADH-coupled assay (34) in a buffer containing 25 mM HEPES, 25 mM KCl, and 4 mM $MgCl_2$. The myosin concentration was 0.25–1 μM. NADH oxidation was followed using the change in absorption at 340 nm in a Beckman DU-650 spectrophotometer. The values for k_{cat} and K_{app} were calculated from fitting the data to the Michaelis-Menten equation. The apparent second order rate constant for actin binding (k_{cat}/K_{app}) was obtained from the calculated ratio of both values. Additionally, at concentrations of actin much lower than K_{app}, the data were fitted to a straight line, and k_{cat}/K_{app} was determined from the slope of this line. The transient kinetics data were interpreted as described previously (27, 29, 34, 35).

RESULTS

Actin Activation of ATPase and Motor Activity Is Dependent on TEDS Phosphorylation—To investigate the regulation of myosin-ID by TEDS site phosphorylation, we used mutant constructs in which the serine at the TEDS site was mutated to either glutamate or alanine to mimic the phosphorylated and dephosphorylated states of the protein.

The steady-state ATPase activity was measured using motor domain construct D692 with TEDS site mutations S332A and S332E. Wild-type and mutant constructs could be purified in sufficient quantities for detailed kinetic analysis. In the absence of actin filaments, all of the constructs displayed similar ATPase activity. To determine the maximum values of the ATPase activity and the efficiency of coupling between actin and nucleotide binding, we measured the ATPase rates with actin concentrations in the range of 0–60 μM F-actin (Fig. 1*A*). The parameters k_{cat}, K_{app}, and k_{cat}/K_{app} were obtained by fitting the data to the Michaelis-Menten equation. They are presented in Table I. K_{app} is the apparent dissociation equilibrium constant for actin binding in the presence of ATP, and k_{cat} gives the maximum value of the ATPase activity. The apparent second order rate constant for actin binding (k_{cat}/K_{app}) indicates the coupling efficiency between actin and nucleotide binding. The ATPase activity of D692(S332A) was only slightly activated by the addition of F-actin. In contrast the ATPase activity of D692(S332E) was strongly activated by actin and showed a hyperbolic dependence on actin concentration. The coupling efficiency of D692(S332E) is 80 times higher than that of the Ser-to-Ala mutants.

Motor function was analyzed directly by measuring the average gliding velocity of actin filaments in an *in vitro* motility assay (26). To investigate the regulation of myosin-ID by TEDS site phosphorylation, we treated the purified D692–2R motor domain constructs with λ-phosphatase to generate the dephosphorylated form or with myosin-I kinase (12) to generate the phosphorylated form. Additionally, we used D692–2R constructs in which the serine at the TEDS site was mutated to either glutamate or alanine.

For each construct, the movement of at least 50 filaments was followed, and the velocity was determined. The average sliding velocities are summarized in Table II. The phosphorylated form of D692–2R showed an average velocity of 890 nm s^{-1}, whereas the dephosphorylated protein displayed no detectable motile activity. Most filaments stayed on the assay surface after the addition of Mg^{2+}ATP. Similar changes in motile activity were observed for the TEDS site mutants. The Ser-to-Glu mutant moved actin filaments with an average velocity of 670 nm s^{-1}, 13-fold faster than the Ser-to-Ala mutant.

TEDS Site Phosphorylation Stabilizes the Acto·Myosin-ID Complex—The rate of actin binding was measured following the exponential decrease in pyrene fluorescence observed on binding of an excess of pyrene-actin to the myosin-ID constructs. The observed rate constants were plotted against pyrene-actin concentration, and the k_{obs} values were linearly dependent upon actin concentration over the range studied (Fig. 1*B*). The second order rate constants of pyrene-actin binding (k_{+A}) were obtained from the slope of the plot, and the resulting values are summarized in Table III. A 3-fold decrease in k_{+A} was observed for D692(S332E) compared with the Ser-to-Ala mutant.

The rate constant for actin dissociation (k_{-A}) was determined by chasing pyrene-actin with a 40-fold excess of unlabeled actin (Fig. 1*C*). The observed process could be fitted to a single exponential, where k_{obs} corresponds directly to k_{-A}. In contrast to their similar rates of actin binding, the mutant constructs displayed significant differences in the rates of actin dissociation. Actin dissociates 30 times faster from D692(S332A) than from the Ser-to-Glu mutant. The dissociation equilibrium constant for actin binding (K_A), as calculated from the ratio of k_{-A} and k_{+A}, indicates an 11-fold increased actin affinity for D692(S332E) compared with the Ser-to-Ala mutant (Scheme 1).

Binding of Nucleotide to Myosin-ID—The rate constants measured for nucleotide binding to wild-type constructs and to TEDS site mutants were mostly identical. Therefore, although all of the measurements were performed with wild-type and mutant constructs, we will refer in most instances only to the wild-type construct.

Rates of ATP binding (K_1k_{+2}) and ADP binding (k_{-6}/K_7) were monitored from the increase in intrinsic protein fluorescence following the addition of excess ATP or ADP (Scheme 2). The observed increases in intrinsic protein fluorescence were 10 and 14% for ADP and ATP binding, respectively. Myosin-ID has the conserved tryptophan in the relay loop, which reports the open to closed transition of Switch II that accompanies ATP hydrolysis (36). Additionally, we measured the binding of the nucleotide analogues 2′(3′)-*O*-(*N*-methylanthraniloyl)-adenosine 5′-triphosphate and 2′(3′)-*O*-(*N*-methylanthraniloyl)-adenosine 5′-diphosphate by following the fluorescence enhancement after mixing with the D692 motor domain constructs. The results of these measurements were analyzed as described previously (30) and are summarized in Table IV. Our

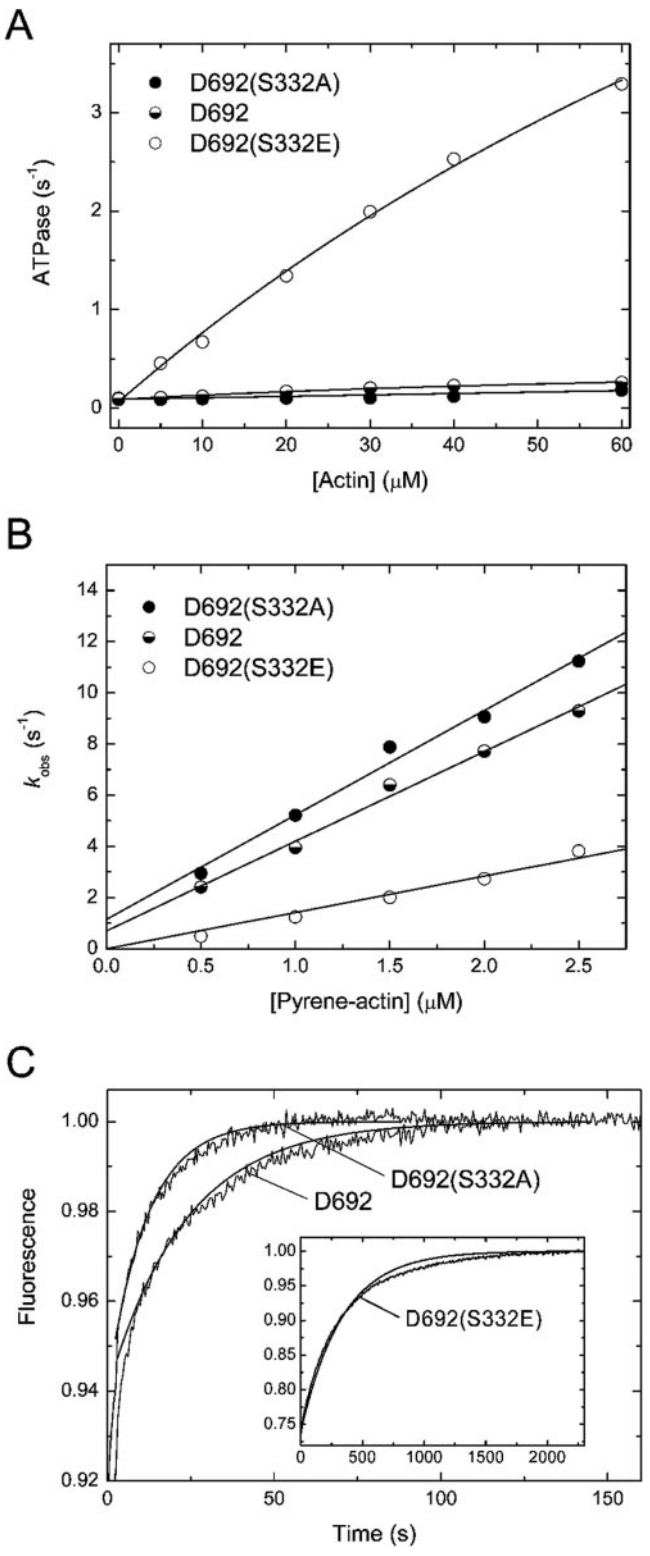

FIG. 1. **Interaction of myosin-ID with F-actin.** *A*, actin stimulation of the steady-state ATPase activities of D692(S332A), D692, and D692(S332E). *B*, interaction of the actin-bound protein with nucleotides and ATP-induced dissociation of pyr-acto·D692. At low ATP concentrations k_{obs} was linearly dependent upon [ATP], and the slopes define the second order binding K_1k_{+2}. In each case the intercept was not significantly different from zero. The symbols correspond to the following constructs D692(S332A) (*filled circle*), D692 (*half-filled circle*), and D692(S332E) (*open circle*). *C*, stopped flow records of the increase in pyrene fluorescence during the pyr-actin displacement of 0.5 μM of the pyr-acto·D692 complex with 20 μM unlabeled actin. The best fits to a single exponential are superimposed with k_{obs} = 0.0027, 0.0430, and 0.0872 s^{-1} for D692(S332A), D692, and D692(S332E), respectively.

results show that for myosin-ID the apparent second order association rate constants (K_1k_{+2} or k_{-6}/K_7) are similar for ATP, ADP, and the mant analogues. At high ATP concentrations the rate of binding saturates for D692 at 640 s^{-1}. For most myosins this maximum rate constant has been attributed to the rate constant for the ATP hydrolysis step ($k_{+3} + k_{-3}$), which is signaled by the fluorescence change of the tryptophan located at the tip of the relay loop (36).

As mentioned above, ATP binding to myosin-ID constructs produced a larger fluorescence increase than the binding of ADP. Therefore, the displacement of ADP by ATP could be followed from the net increase in fluorescence upon displacement of excess ADP from the D692-ADP complex by the addition of a larger excess ATP. The rate of ADP release from D692 (k_{+6}) was 0.60 s^{-1}. At intermediate ADP concentrations (<40 μM), the reaction observed on adding excess ATP to D692 could be described by two exponentials. The amplitude of the fast phase declined, and that of the slow phase increased with increasing ADP. The fast process is the rate at which ATP binds to unliganded myosin (K_1k_{+2}[ATP]), and the slow process is the rate at which ATP replaces ADP bound to myosin (k_{+6}). Accordingly the slow phase was independent of the concentration of ATP used. The dependence of the amplitudes on the ADP concentration was described by hyperbolic functions, which define the equilibrium constant of ADP binding to D692 (K_6K_7). The value obtained for D692 was 1.9 μM (Table IV).

Nucleotide Binding to Acto·Myosin-ID—The binding of ATP to the acto·myosin-ID complex could be followed by observing the exponential increase in fluorescence of pyrene-actin, because the complex formed by F-actin and D692 dissociates following the addition of excess ATP. The observed rate constants were linearly dependent upon ATP concentration in the range of 5–25 μM (Fig. 2*A*). The apparent second order binding constant K_1k_{+2} (Scheme 3) is defined by the gradient of the plot. Values of 0.49 μM^{-1} s^{-1} were obtained for D692, and similar values were obtained with the mutant constructs. At high ATP concentrations (>2 mM), the observed rate constants saturate, and the dependence on the ATP concentration could be described by a hyperbola, where the maximum value of k_{obs} defines k_{+2} (Fig. 2*A*, *inset*).

The affinity of ADP for the complex formed by the myosin-ID motor domain and F-actin (K_{AD}) was determined from the inhibition of the ATP-induced dissociation of acto·D692 by ADP. The observed rate of dissociation was reduced for all constructs when excess ATP was added to acto·D692 in the presence of varying concentrations of ADP. The reaction was monophasic for D692, which is compatible with a fast equilibrium for ADP binding (Fig. 2*B*). The observed rate constants were plotted against the ADP concentration, and the data were fitted with a hyperbola (Fig. 2*C*). Dissociation constants (K_{AD}) of 75 and 118 μM were obtained for D692(S332E) and D692(S332A), respectively. In the case of D692(S332A), binding of ADP to the actomyosin complex caused dissociation of actin from the complex, consistent with a low actin affinity, which is predicted to be 500 nM in the presence of saturating ADP for this construct.

The Motile Activity of Myosin-ID Is Inhibited by Free Mg^{2+} Ions—Actin gliding velocities, as described above, were determined under the standard conditions for the *in vitro* motility assay, as established for myosin-II and now commonly used for the analysis of all myosin constructs. To test whether these conditions are appropriate for the analysis of class I myosins, we performed a series of assays under nonstandard conditions where either the $MgCl_2$ concentration was kept constant and the ATP concentration was changed or the $MgCl_2$ concentration was changed and the ATP concentration kept constant. The results of

TABLE I
Actin activation of ATPase activity

The experimental conditions were 25 mM HEPES, pH 7.4, 25 mM KCl, and 4 mM $MgCl_2$ at 25 °C.

Myosin construct	ATPase activity[a]			Michaelis-Menten parameters[b,c]		
	Basal	Activated	Activation	k_{cat}	K_{app}	k_{cat}/K_{app}
	s^{-1}	s^{-1}		s^{-1}	μM	$\mu M^{-1}\ s^{-1}$
D692(S332A)	0.09 ± 0.01	0.10 ± 0.02	0.1	ND[d]	ND	0.001
D692	0.12 ± 0.02	0.17 ± 0.03	0.3	ND	ND	0.004
D692(S332E)	0.10 ± 0.02	1.34 ± 0.10	12.4	10.0 ± 3.0	130 ± 50	0.077
M765	0.08 ± 0.01	0.68 ± 0.09	7.5	2.6 ± 0.4	73 ± 20	0.036

[a] Actin-activated ATPase activity was measured in the presence of 20 μM rabbit skeletal muscle F-actin. ATPase activation = (actin-activated ATPase − basal ATPase)/basal ATPase.
[b] The values for k_{cat} and K_{app} were calculated from fitting the data to the Michaelis-Menten equation.
[c] The apparent second order rate constant for actin binding (k_{cat}/K_{app}) was obtained from the calculated ratio of both values. Alternatively the data at concentrations of actin much lower than K_{app} could be fit to a straight line, and k_{cat}/K_{app} was determined from the slope of this line.
[d] ND, not determined.

TABLE II
Motile activity of myosin-ID constructs

	Average sliding velocity[a,b]	
	D692–2R	M765–2R
	$\mu m/s$	
Untreated	0.13 ± 0.04	0.82 ± 0.07
Phosphatase-treated	No motility	NA[e]
Kinase-treated	0.89 ± 0.10	NA
S332A	0.05 ± 0.02	NA
S332E	0.67 ± 0.09	NA
High [ATP][c]	1.78 ± 0.20[d]	0.83 ± 0.08

[a] The uncertainties represent standard deviations of the mean values.
[b] The experimental conditions were 2 mM ATP, 4 mM $MgCl_2$, 25 mM imidazole, pH 7.4, 25 mM KCl, 1 mM EGTA, and 10 mM dithiothreitol at 30 °C.
[c] The experimental conditions were 10 mM ATP, 4 mM $MgCl_2$, 25 mM imidazole, pH 7.4, 25 mM KCl, 1 mM EGTA, and 10 mM dithiothreitol at 30 °C.
[d] Measured for D692–2R(S332E).
[e] NA, not applicable.

TABLE III
Actin affinity

Treatment of the TEDS site mutant constructs with apyrase did not result in significant changes in the observed rate constants. K_A, K_{AD}, and K_D are defined as dissociation equilibrium constants. The experimental conditions were 20 mM MOPS, pH 7.0, 5 mM $MgCl_2$, and 100 mM KCl at 20 °C.

Myosin construct	k_{+A}	k_{-A}	K_A
	$\mu M^{-1}\ s^{-1}$	ms^{-1}	nM
D692	3.5 ± 0.2	43.0 ± 0.7	12.3
D692(S332A)	4.1 ± 0.3	87.2 ± 1.9	21.1
D692(S332E)	1.4 ± 0.1	2.7 ± 0.2	1.9
M765	0.8 ± 0.1	2.2 ± 0.2	2.9

these experiments show that at optimal Mg^{2+} ion concentrations the average sliding velocity of D692–2R(S332E) is more than 5-fold faster than that of the Ser-to-Ala mutant. Furthermore, at optimal Mg^{2+} concentrations, the average sliding velocity for constructs D692–2R(S332E) and D692–2R(S332A) is 3-fold faster than under standard assay conditions.

When the $MgCl_2$ concentration was kept constant, the average sliding velocities of both D692–2R(S332E) and D692–2R(S332A) displayed a sigmoidal dependence on ATP concentration, and the data were best described by the Hill equation. Average sliding velocities increased with increasing ATP concentrations from 42 to 325 nm s^{-1} for D692–2R(S332A) and from 500 to 1720 nm s^{-1} for D692–2R(S332E) (Fig. 3*A*). The midpoint of the titration coincided in every case with near equimolar concentrations of ATP and Mg^{2+} ions, indicating that binding of Mg^{2+} ions by ATP may overcome an inhibitory effect of free Mg^{2+} ions on motile activity.

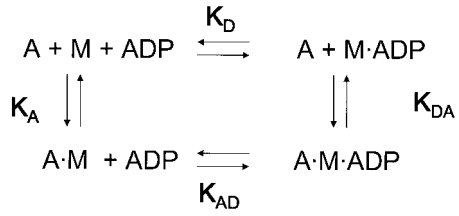

SCHEME 1

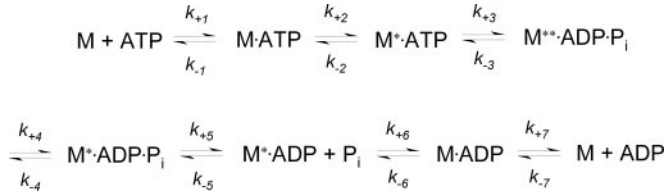

SCHEME 2

Data from titrations performed in the presence of 1–20 mM ATP were used to determine the dependence of the average sliding velocity of the constructs on the concentration of free Mg^{2+} ions. In the presence of millimolar concentrations of ATP and submicromolar concentrations of free Mg^{2+} ions, both D692–2R(S332E) and D692–2R(S332A) moved actin filaments with a velocity of 250–300 nm s^{-1}. In the presence of free Mg^{2+} ion concentrations up to 0.2 mM, the Ser-to-Ala mutant continued to move F-actin with a velocity of ~300 nm s^{-1}. In contrast, the motile activity of the Ser-to-Glu mutant displayed a 6-fold increase, reaching a plateau value of 1700 nm s^{-1} at a free Mg^{2+} ion concentration of 0.1 mM. The data were again best described by the Hill equation (Fig. 3*B*).

At free Mg^{2+} ion concentrations above 0.4 mM, sharp reductions in motile activity from ~1700 to 500 nm s^{-1} and from 300 to 40 nm s^{-1} were observed for Ser-to-Glu and Ser-to-Ala constructs, respectively. Further titrations showed that the midpoints of the sigmoidal curves describing the drop in motile activity again coincided with close to equimolar concentrations of ATP and $MgCl_2$. The myosin II-base construct M765–2R showed no changes in motile activity under the same conditions (Table II). Additionally, we confirmed that the observed changes in average sliding velocity are not due to changes in ionic strength. The Ser-to-Glu construct showed no reduction in motile activity even at twice the ionic strength used for these experiments, whereas the Ser-to-Ala construct started to show a marked reduction at only slightly higher ionic strength. All of the data points shown in *panels C* and *D* of Fig. 3 were measured at lower ionic strength than the data point at 20 mM ATP in Fig. 3*A*. Finally, increasing the Ca^{2+} ion instead of the Mg^{2+} ion concentration did not lead to a reduction in motile activity.

TABLE IV
Rate and equilibrium constants of nucleotide binding to myosin and acto·myosin complexes
For comparison, the parameters obtained for *D. discoideum* myosin II motor domain fragment M765 are shown.

Nucleotide	Rate constant	D692	M765
Nucleotide binding to myosin			
ATP	K_1k_2 (μM^{-1} s^{-1})	0.66 ± 0.01	0.56 ± 0.03
	k_{max} (s^{-1})	640 ± 10	30 ± 1
mantATP	K_1k_2 (μM^{-1} s^{-1})	0.53 ± 0.02	0.81 ± 0.02
ADP	k_{-6}/K_7 (μM^{-1} s^{-1})	0.98 ± 0.02	No signal
	k_{+6} (s^{-1})	0.60 ± 0.002	No signal
	K_D (μM)[a]	1.9 ± 0.3 (0.6)	(14)[b]
mantADP	k_{-6}/K_7 (μM^{-1} s^{-1})	0.87 ± 0.01	0.36 ± 0.004
Nucleotide binding to acto· myosin			
ATP	K_1k_{+2} (μM^{-1} s^{-1})	0.49 ± 0.01	0.16 ± 0.002
	k_{+2} (s^{-1})	960 ± 20	490 ± 20
ADP[c]	K_{AD} (μM)	75 ± 4	253 ± 11
	K_{AD}/K_D	40	18

[a] The values are derived from biphasic ADP dissociation reactions at different ADP concentrations for D692–2R(S332E). The value in parentheses is obtained from the calculated $k_{+6}/(k_{-6}/K_7)$.
[b] Ref. 29.
[c] The values refer to the Ser-to-Glu mutants of the myosin-I motor domain constructs. The K_{AD} value for D692(S332A) is 118 μM. K_{AD} and K_D are defined as dissociation equilibrium constants. The experimental conditions were 20 mM MOPS, pH 7.0, 5 mM $MgCl_2$, and 100 mM KCl at 20 °C.

To elucidate how changes in the free Mg^{2+} concentration affect the ATPase cycle of myosin-ID, we examined the release of ADP from actomyosin by repeating the experiments of Fig. 2*C* at a range of added Mg^{2+} concentrations from 0 to 20 mM. For D692 the value of K_{AD} dropped from 134 ± 28 μM at 0 mM Mg^{2+} to 70 ± 2 μM at 20 mM Mg^{2+} (Fig. 4). An apparent Mg^{2+} binding constant of 0.3 mM can be estimated from these results. Therefore our data indicate that elevated Mg^{2+} concentrations can inhibit ADP release by about 2-fold for myosin-ID.

For completeness, we also examined the effect of free Mg^{2+} ions on the rate of ADP release from myosin-ID in the absence of actin. We determined an apparent affinity for Mg^{2+} ions of 0.3 mM. Higher Mg^{2+} ion concentrations lead to a 7–8-fold inhibition of the rate of ADP release.

DISCUSSION

The direct functional characterization of the vast majority of myosins is greatly impeded because their respective light chains have not been identified. In the case of class I myosins, analysis of the motor activity of the native protein is further hampered by the presence of an ATP-insensitive actin-binding site in the tail region. The direct fusion of an artificial lever arm to the motor domain overcomes both these problems. The kinetic properties of the resulting constructs are not affected by the fusion, and their velocity can be compared with reference constructs derived from conventional myosin (38, 39).

Here, we show that myosin-ID is a fast ATPase and possesses the ability to translocate actin filaments at greater velocities than comparable myosin-II constructs. Steady-state kinetic measurements demonstrate that the presence of a negative charge at the TEDS site increases the ability of actin to stimulate ATPase activity. Both the maximum turnover rate (k_{cat}) and the apparent second order binding constant for F-actin (k_{cat}/K_{app}), which is a measure of the coupling efficiency between actin binding and ATP-turnover, are increased. The results of our transient kinetics experiments show that charge changes at the TEDS site do not affect the interactions between the myosin motor and nucleotides, but the presence of a negative charge is important to stabilize the actomyosin complex. This is primarily due to a stabilization of bound F-actin via a 30-fold reduction in the actin off-rate (k_{-A}). Similar effects have been observed following the introduction of a single negative charge in the actin-binding region of myosin-II (34).

D. discoideum Myosin-ID and Myosin II Show Similar Properties—The activated forms of the myosin-ID constructs D692 and D692–2R display kinetic and functional properties that are very similar to those of the genetically engineered myosin II constructs M765 and M765–2R, the values for basal ATPase activity, k_{cat}/K_{app} and maximal motility all differing by less than a factor of 2. Similar, the affinity for F-actin and the second order rate constants for ATP and ADP binding are within a factor of 2 of the values for M765. Larger differences are observed in the maximal rate of the fluorescence change on ATP binding to myosin, which is 10-fold faster for myosin-ID than M765. If this reflects in both cases the closing of Switch II and the hydrolysis step, then it suggests that the recovery stroke of the cross-bridge cycle is much faster for myosin-ID than for myosin II. This difference may reflect the need for the single headed myosin to recover more quickly from detachment and rebind faster to the actin. The high value of the rate of this fluorescence change is similar to that seen in the processive myosin V. However, the low K_{app} for actin and the low basal ATPase rates are consistent with the myosin ADP·P_i state being the predominant steady-state intermediate and myosin-ID being a low duty ratio motor.

The ADP affinity is ~2 μM, similar to many other myosins, but tighter than 14 μM, as recorded for M765. K_{AD} is 3-fold tighter than for M765, suggesting a lower rate of ADP release from acto-myosin, but this is compensated for by a 3-fold faster rate of ATP binding to acto-myosin. For fast type myosins the velocity of movement is often limited by the rate at which the cross-bridge detaches after completion of the working stroke. This step is limited by both the rate of ADP release from the cross-bridge and the rate of ATP binding (33, 40). The overall net rate of cross-bridge detachment may therefore be about the same for these two motors, consistent with the similar measured maximal velocities.

Regulation of Myosin-ID by Mg^{2+} Ions—In addition to the regulation by TEDS site phosphorylation, our results indicate a Mg^{2+} ion-dependent mechanism that controls the motile activity of myosin-ID. Like all other myosins, myosin-ID is only an active motor in the presence of Mg^{2+} ions. Both in the case of the phosphorylated and dephosphorylated protein, submicromolar concentrations of Mg^{2+} ions are sufficient to promote a basal motor activity of ~250 nm s^{-1}. The increase in motile activity from 300 to 1700 nm s^{-1}, displayed by D692–2R (S332E) in the presence of free Mg^{2+} ion concentrations greater than 1 μM, appears to correlate with the binding of Mg^{2+} ions to ATP in solution. The equilibrium dissociation constants for Mg^{2+} binding to ATP is 87 μM (42). Therefore, at Mg^{2+} ion concentrations below 100 μM and ATP concentrations in the

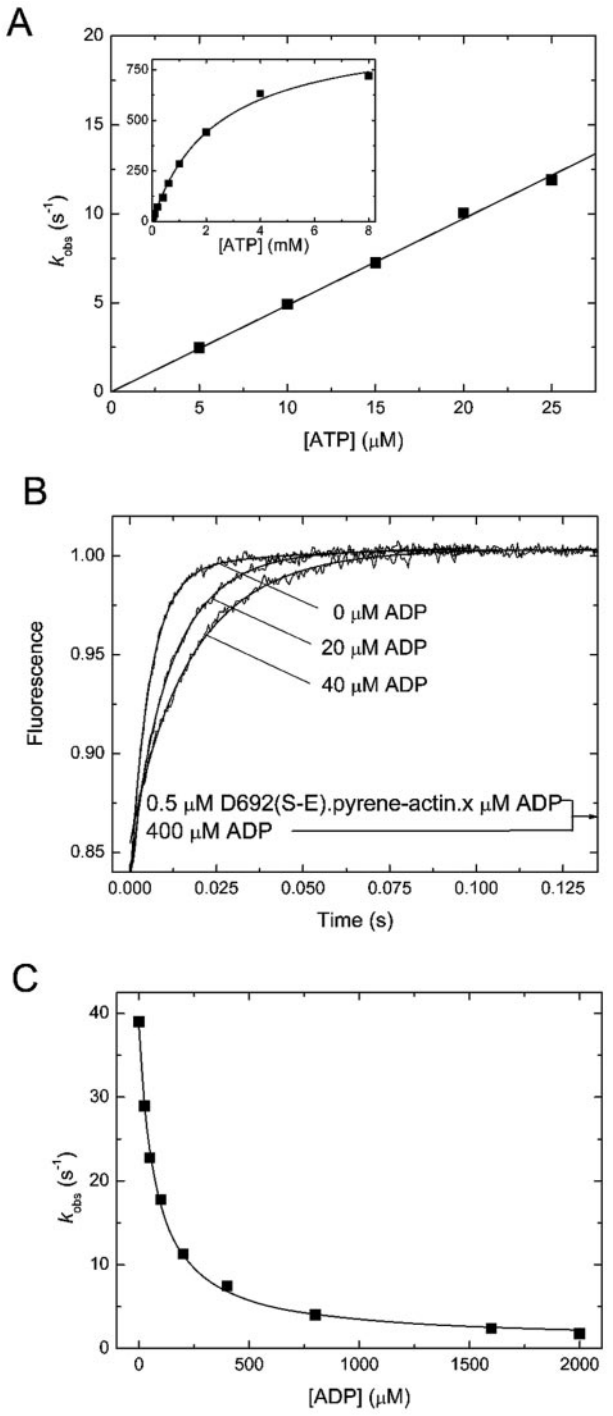

FIG. 2. **Transient kinetic analysis of the interaction of myosin-ID with actin and nucleotides.** *A*, ATP-induced dissociation of the actomyosin complex. The observed rate constant for D692 is linearly dependent on the ATP concentration in the range 5–25 μM. The apparent second order rate constant for ATP binding to actomyosin (K_1k_{+2}) was determined from the slope of the line. The *inset* shows data over the range from 0.005 to 8 mM fitted to a hyperbola. The rate constants for the isomerization step are given by the plateau values. *B*, ADP inhibition of ATP-induced dissociation of the actomyosin complex of D692(S332E). Monophasic dissociation reactions are observed in the presence of different amounts of ADP, compatible with a fast equilibrium for ADP binding. *C*, the observed rate constants were plotted against the ADP concentration, and the data were fitted with a hyperbola.

millimolar range, the observed slower velocities may result from ATP competing effectively with Mg^{2+}-ATP for the nucleotide-binding site of myosin-ID.

$$A{\cdot}M + ATP \underset{}{\overset{K_1}{\rightleftharpoons}} A{\cdot}M{\cdot}ATP \xrightarrow{k_{+2}} A + M{\cdot}ATP$$

$$A{\cdot}M{\cdot}ADP \overset{K_{AD}}{\rightleftharpoons} A{\cdot}M + ADP$$

SCHEME 3

Additionally, all of the myosin-ID constructs display a strong inhibition of actin sliding velocity by free Mg^{2+} ions in the range from 0.3 to 1.5 mM. These results are in good agreement with a model that requires the coordination of the Mg^{2+} ion with protein and ADP to be broken before ADP can be released. Changes in the free Mg^{2+} ion concentrations can then act to shift the equilibrium from the free to the bound complex by simple mass action. The sharp reduction in motility, which is observed at free Mg^{2+} ion concentrations greater than 0.3 mM (Fig. 3, *C* and *D*), can be explained by this model and is consistent with the results of our transient kinetic measurements. Both sets of experiments indicate that free Mg^{2+} ions inhibit myosin-ID activity with a K_i of ~1 mM.

The absence of a rise in the motile activity of D692–2R (S332A), when the Mg^{2+} ion concentration is increased from 0.1 to 2 mM, can be explained if actin binding is perturbed by the absence of a negative charge at the TEDS site. As a result of this perturbation, the coupling efficiency between actin binding and ATP turnover (k_{cat}/K_{app}) is 80-fold lower for D692–2R(S332A) than for the Ser-to-Glu mutant. Therefore, the release of phosphate is likely to become the rate-limiting step for D692–2R(S332A). The reduced motile activity at free Mg^{2+} ion concentrations greater than 0.1 mM (Fig. 3*D*) can be explained by free Mg^{2+} ions inhibiting the release of ADP, as observed for D692–2R(S332E). The actin-activated ATPase of the Ser-to-Ala construct is barely above the basal level, and P_i release is clearly rate-limiting for ATP hydrolysis. However, this does not mean that P_i release limits motile activity. Our results indicate that the Ser-to-Ala mutant has a very low actin affinity for the myosin ADP·P_i state. Therefore, productive interactions with actin are rare, but once such a productive interaction does occur the cycle may be reasonably normal. The motility of the constructs is thus the result of a small number of productive interactions with actin, with those few productive cross-bridges experiencing Mg^{2+} inhibition of ADP release similar to that observed for the Ser-to-Glu construct.

Removal of the phosphate group from the TEDS site and inhibition by free Mg^{2+} ions can combine to achieve a more than 40-fold reduction in velocity. However, although both the removal of the TEDS site phosphate and inhibition by free Mg^{2+} ions reduce steady-state ATPase activity and sliding velocity, their consequences for myosin-ID motor activity are quite different. Although the first perturbs actin binding and leads to the accumulation of the weak binding myosin ADP·P_i intermediate, the latter leads to the accumulation of the strong binding actin myosin ADP intermediate. In consequence, the modification at the TEDS site acts like a general on/off switch, whereas changes in the concentration of free Mg^{2+} ions reduce the ability of the motor to produce fast movement but increase its capacity for bearing tension. The difference between the motor activities of the phospho- and dephospho-protein is certainly more pronounced *in vivo*, because the load on the motor is close to zero in our *in vitro* assay.

Additionally, Mg^{2+} binding to the myosin-ID light chain (MlcD) may act by modifying lever arm stiffness and thus adding a further level of Mg^{2+} ion-dependent regulation of myosin-ID motor activity. Côté and co-workers (43) have shown that MlcD undergoes a conformational change upon binding of

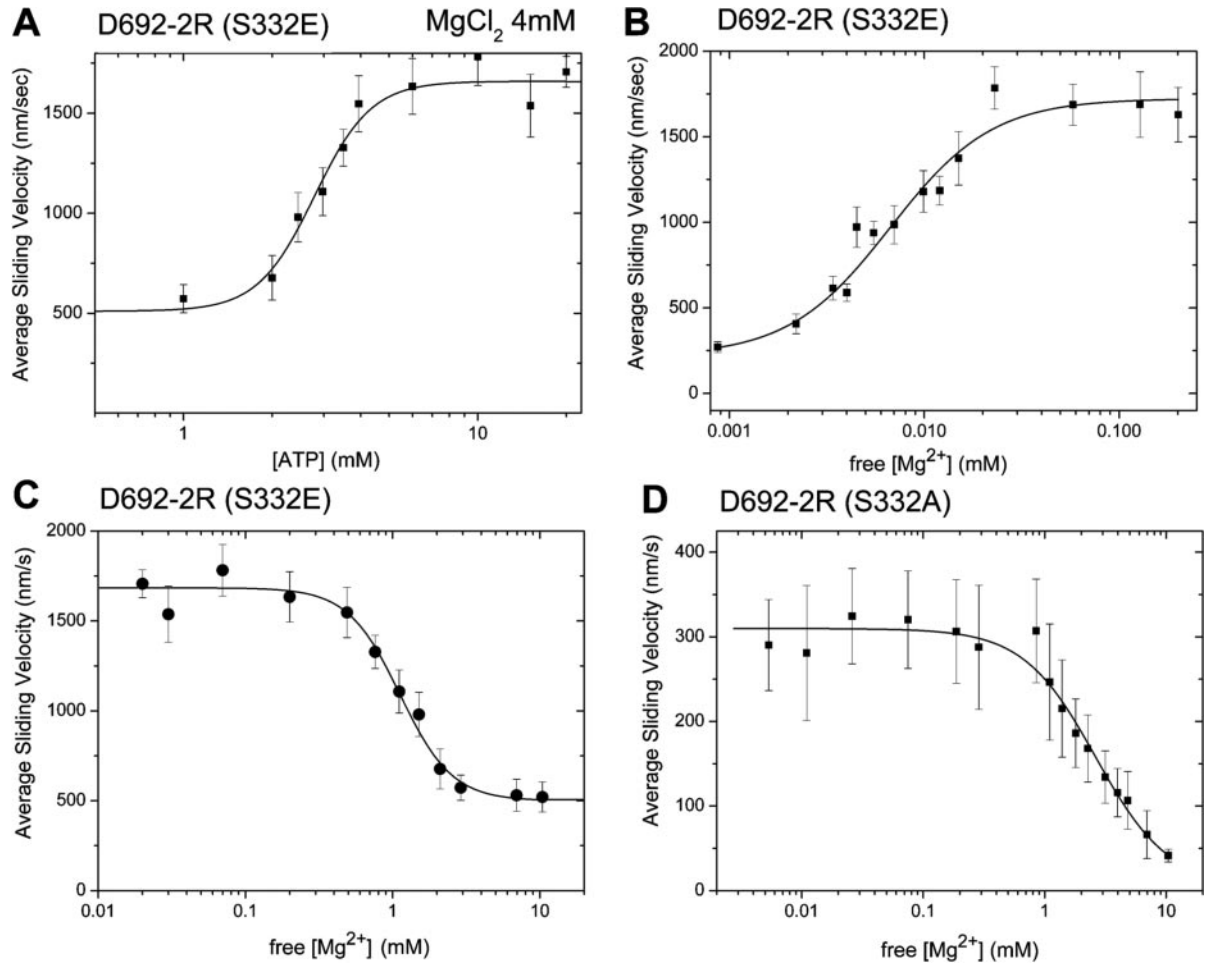

FIG. 3. **Myosin-ID motor activity is inhibited by free Mg^{2+} ions.** *A*, ATP titration of D692–2R(S332E) motor activity in the presence of 4 mM. The $MgCl_2$ concentration is kept constant at 4 mM, and the ATP concentration is varied in the range from 0.5 to 20 mM. *B*, D692–2R(S332E) motor activity in the presence of 1 μM to 2 mM free Mg^{2+} ions. *C*, D692–2R(S332E) motor activity in the presence of 20 μM to 10 mM free Mg^{2+} ions. *D*, D692(S332A) motor activity in the presence of 60 μM to 10 mM free Mg^{2+} ions. Free Mg^{2+} ion concentrations were calculated using Maxchelator software (37). The experimental conditions were 25 mM imidazole, pH 7.4, 25 mM KCl, 1 mM EGTA, and 10 mM dithiothreitol at 30 °C.

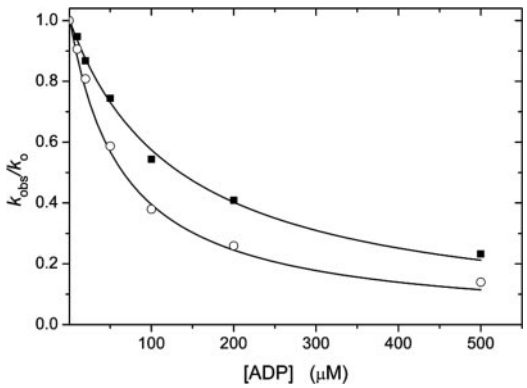

FIG. 4. **Inhibition of the rate of ADP release from acto·D692–2R(S332E) by free Mg^{2+} ions.** Normalized rate constants were plotted against the ADP concentration, and the data were fitted with a hyperbola. The values for K_{AD} determined in the presence of 0.2 (■) and 5 mM (○) $MgCl_2$ were 132 and 72 μM, respectively. The experimental conditions were 20 mM MOPS, pH 7.0, 5 mM $MgCl_2$, and 100 mM KCl at 20 °C.

Mg^{2+} ions, which can be detected as a change in tryptophan fluorescence intensity. The MlcD has only a low affinity for Ca^{2+} ions and a K_d for Mg^{2+} ions of ~450 μM. Thus, the occupancy of the metal-binding site of MlcD and the coordination of the Mg^{2+} ion at the nucleotide-binding site are equally responsive to changes that lie within the range of physiological free Mg^{2+} ion concentrations in *D. discoideum* and many other cell types (41, 42, 44).

Inhibition of ADP release by free Mg^{2+} ions has not been observed for the extensively studied class II myosins, and therefore *in vitro* motility assays are commonly performed in the presence of a millimolar excess of Mg^{2+} over ATP. Therefore, inhibition by free Mg^{2+} ions may have masked the fast motor activity of unconventional myosins in other studies. Additionally, changes in the concentration of Mg^{2+} ions may play a more general role in modulating the motor activity of unconventional myosins.

Acknowledgments—We thank S. Zimmermann and R. Schumann for excellent technical assistance, E. D. Korn and H. Brzeska for providing myosin-I heavy chain kinase; and I. Chizhov, G. Tsiavaliaris, and J. Wray for help and discussion.

REFERENCES

1. Mermall, V., Post, P. L., and Mooseker, M. S. (1998) *Science* **279,** 527–533
2. Doberstein, S. K., and Pollard, T. D. (1992) *J. Cell Biol.* **117,** 1241–1249
3. Miyata, H., Bowers, B., and Korn, E. D. (1989) *J. Cell Biol.* **109,** 1519–1528
4. Lynch, T. J., Brzeska, H., Miyata, H., and Korn, E. D. (1989) *J. Biol. Chem.* **264,** 19333–19339
5. Jung, G., and Hammer, J. A., III (1994) *FEBS Lett.* **342,** 197–202
6. Lynch, T. J., Albanesi, J. P., Korn, E. D., Robinson, E. A., Bowers, B., and Fujisaki, H. (1986) *J. Biol. Chem.* **261,** 17156–17162
7. Titus, M. A., Wessels, D., Spudich, J. A., and Soll, D. (1993) *Mol. Biol. Cell* **4,** 233–246
8. Geli, M. I., Lombardi, R., Schmelzl, B., and Riezman, H. (2000) *EMBO J.* **19,** 4281–4291
9. Bement, W. M., and Mooseker, M. S. (1995) *Cell Motil. Cytoskel.* **31,** 87–92
10. Brzeska, H., Young, R., Tan, C., Szczepanowska, J., and Korn, E. D. (2001) *J. Biol. Chem.* **276,** 47468–47473

11. Wu, C., Lee, S. F., Furmaniak-Kazmierczak, E., Cote, G. P., Thomas, D. Y., and Leberer, E. (1996) *J. Biol. Chem.* **271,** 31787–31790
12. Brzeska, H., Young, R., Knaus, U., and Korn, E. D. (1999) *Proc. Natl. Acad. Sci. U. S. A.* **96,** 394–399
13. Lee, S. F., Mahasneh, A., de la Roche, M., and Cote, G. P. (1998) *J. Biol. Chem.* **273,** 27911–27917
14. Buchwald, G., Hostinova, E., Rudolph, M. G., Kraemer, A., Sickmann, A., Meyer, H. E., Scheffzek, K., and Wittinghofer, A. (2001) *Mol. Cell. Biol.* **21,** 5179–5189
15. Anson, M., Geeves, M. A., Kurzawa, S. E., and Manstein, D. J. (1996) *EMBO J.* **15,** 6069–6074
16. Kliche, W., Fujita-Becker, S., Kollmar, M., Manstein, D. J., and Kull, F. J. (2001) *EMBO J.* **20,** 40–46
17. Brzeska, H., Szczepanowska, J., Hoey, J., and Korn, E. D. (1996) *J. Biol. Chem.* **271,** 27056–27062
18. Wang, Z. Y., Wang, F., Sellers, J. R., Korn, E. D., and Hammer, J. A., III (1998) *Proc. Natl. Acad. Sci. U. S. A.* **95,** 15200–15205
19. De La Cruz, E. M., Ostap, E. M., and Sweeney, H. L. (2001) *J. Biol. Chem.* **276,** 32373–32381
20. Faulstich, H., Trischmann, H., and Mayer, D. (1983) *Exp. Cell Res.* **144,** 73–82
21. Watts, D. J., and Ashworth, J. M. (1970) *Biochem. J.* **119,** 171–174
22. de Hostos, E. L., Bradtke, B., Lottspeich, F., Guggenheim, R., and Gerisch, G. (1991) *EMBO J.* **10,** 4097–4104
23. Bain, G., and Tsang, A. (1991) *Mol. Gen. Genet.* **226,** 59–64
24. Manstein, D. J., Schuster, H. P., Morandini, P., and Hunt, D. M. (1995) *Gene* (*Amst.*) **162,** 129–134
25. Knetsch, M. L., Tsiavaliaris, G., Zimmermann, S., Ruhl, U., and Manstein, D. J. (2002) *J. Mus. Res. Cell Motil.* **23,** 605–611
26. Kron, S. J., and Spudich, J. A. (1986) *Proc. Natl. Acad. Sci. U. S. A.* **83,** 6272–6276
27. Cremo, C. R., and Geeves, M. A. (1998) *Biochemistry* **37,** 1969–1978
28. Furch, M., Fujita-Becker, S., Geeves, M. A., Holmes, K. C., and Manstein, D. J. (1999) *J. Mol. Biol.* **290,** 797–809
29. Batra, R., Geeves, M. A., and Manstein, D. J. (1999) *Biochemistry* **38,** 6126–6134
30. Kurzawa, S. E., and Geeves, M. A. (1996) *J. Mus. Res. Cell Motil.* **17,** 669–676
31. Bagshaw, C. R., Eccleston, J. F., Eckstein, F., Goody, R. S., Gutfreund, H., and Trentham, D. R. (1974) *Biochem. J.* **141,** 351–364
32. Millar, N. C., and Geeves, M. A. (1983) *FEBS Lett.* **160,** 141–148
33. Siemankowski, R. F., and White, H. D. (1984) *J. Biol. Chem.* **259,** 5045–5053
34. Furch, M., Geeves, M. A., and Manstein, D. J. (1998) *Biochemistry* **37,** 6317–6326
35. Kurzawa, S. E., Manstein, D. J., and Geeves, M. A. (1997) *Biochemistry* **36,** 317–323
36. Batra, R., and Manstein, D. J. (1999) *Biol. Chem.* **380,** 1017–1023
37. Patton, C., Thompson, S., and Epel, D. (2004) *Cell Calcium* **35,** 427–431
38. Ito, K., Kashiyama, T., Shimada, K., Yamaguchi, A., Awata, J., Hachikubo, Y., Manstein, D. J., and Yamamoto, K. (2003) *Biochem. Biophys. Res. Commun.* **312,** 958–964
39. Tsiavaliaris, G., Fujita-Becker, S., and Manstein, D. J. (2004) *Nature* **427,** 558–561
40. Weiss, S., Rossi, R., Pellegrino, M. A., Bottinelli, R., and Geeves, M. A. (2001) *J. Biol. Chem.* **276,** 45902–45908
41. Satre, M., and Martin, J. B. (1985) *Biochem. Biophys. Res. Commun.* **132,** 140–146
42. Michailova, A., and McCulloch, A. (2001) *Biophys. J.* **81,** 614–629
43. de La Roche, M. A., Lee, S. F., and Cote, G. P. (2003) *Biochem. J.* **374,** 697–705
44. Martin, J. B., Foray, M. F., Klein, G., and Satre, M. (1987) *Biochim. Biophys. Acta* **931,** 16–25